H_2 consumption by acetogenic bacteria follows first-order kinetics

Laura Muñoz-Duarte[1] Laura.munoz@bce.au.dk https://orcid.org/0000-0003-0705-9999

Susmit Chakraborty[1], such@bce.au.dk

Louise Vinther Grøn[1] louise.groen@bce.au.dk

Maria Florencia Bambace[1] mfbambace@bce.au.dk

Jacopo Catalano[2] jcatalano@au.dk https://orcid.org/0000-0003-4819-5436

Jo Philips[1]* jo.philips@bce.au.dk https://orcid.org/0000-0003-0471-7802

Department of Biological and Chemical Engineering

Aarhus University

[1]Gustav Wieds vej 10C,

[2] Åbogade 40A,

Aarhus, 8200 Denmark

*Corresponding author (jo.philips@bce.au.dk), Phone: +4593521569

Abstract

Acetogenic bacteria play an important role in various environmental and biotechnological processes, because of their autotrophic metabolism converting carbon dioxide with molecular hydrogen (H_2) as electron donor into acetate. The main factor limiting acetogenesis is often H_2. Assessing the potential of acetogens in environmental and biotechnological processes thus requires insights into their H_2 consumption kinetics. In this study, initial H_2 consumption rates at a range of different initial H_2 concentrations were measured for three different acetogens. Interesting, for all three strains, H_2 consumption was found to follow first-order kinetics, i.e. the H_2 consumption rate increased linearly with the dissolved H_2 concentration up to almost saturated H_2 levels. This contradicts Monod kinetics, which is commonly assumed for acetogens. The obtained first-order rate coefficients (k_1) were further validated by fitting first-order kinetics on previous time-course experimental results. The latter method was also used to determine the k_1 value of five additional acetogens strains. Biomass specific first-order rate coefficients were found to vary up to six-fold, with the highest k_1 for *Acetobacterium wieringae* and the lowest for *Sporomusa sphaeroides*. Overall, our results demonstrate the importance of the dissolved H_2 concentration to understand the rate of acetogenesis in environmental and biotechnological settings.

Keywords

Acetogenic bacteria, H_2 consumption characteristics, first-order kinetics, CO_2 reduction, strain selection, gas fermentation, microbial electrosynthesis.

54 **Synopsis**

55 Acetogenic bacteria are diverse, although they catalyze the same overall reaction. This study
56 provides insights into their different H_2 consumption rates, which has implications for their
57 role in the environment and in biotechnological applications.

Introduction

Acetogens are an interesting group of strictly anaerobic bacteria with remarkable metabolic capabilities. They are phylogenetically diverse, but have the common characteristic of utilizing the Wood–Ljungdahl pathway (WLP) for CO_2 fixation and acetate production while conserving energy, using H_2 as electron donor [1], according to the reaction:

$$4\ H_2 + 2\ CO_2 \rightarrow CH_3COOH + 2\ H_2O \quad \Delta G^{0'} = -95\ \text{kJ/mol} \tag{1}$$

Acetogens are widely distributed across diverse environments, ranging from soils to the human gut [2,3]. In addition, the metabolic abilities of acetogens are attractive for the development of novel biotechnological processes to convert carbon dioxide into valuable products. In gas fermentation, CO_2 is metabolized in a bioreactor fed with H_2 gas, while an electrode is used to produce H_2 *in situ* in the case of microbial electrosynthesis [4]. In these biotechnological settings, as well as in natural environments, the supply of H_2 often limits acetogenesis [5]. Understanding the relationship between the H_2 level and the kinetics of H_2 consumption and acetogenesis is thus essential for assessing the potential of acetogens in biotechnological and environmental processes.

Most often, H_2 consumption and growth by acetogens is assumed to follow Monod kinetics (similar to Michaelis Menten kinetics for enzymes)[5], in which the rate (μ) increases with the substrate concentration *[S]*, until a maximum rate (μ_{max}) is reached [6]:

$$\mu = \mu_{\max} \frac{[S]}{K_s + [S]} \tag{2}$$

The half-saturation coefficient K_s gives the substrate concentration at which half of the maximum rate is reached. So far, (maximum) growth rates or doubling times have frequently

been reported for acetogens[7,8], but only few studies have reported half-saturation coefficients for H_2 consumption by acetogens (**Table 1**). Moreover, not all of these studies carefully characterized whether the relationship between the H_2 consumption rate and the H_2 concentration is well described by Monod kinetics (Eq. 2).

Table 1. Reported values of half-saturation coefficients (K_s) for H_2 consumption by acetogens.

Acetogen	K_s (µM)	Method	Reference
Acetobacterium woodii	0.73	Chemostat; based on half of the max growth rate	[9]
Acetobacterium woodii	2500	Enzyme assay on purified hydrogenases from cells grown on fructose	[15]
Acetobacterium bakii	4	Batch; H_2 depletion curves over time, constant biomass	[10]
Sporomusa termitida	6	Batch without headspace; H_2 depletion in the liquid	[11]
Eubacterium limosum	340	Batch; H_2 depletion curves over time- initial rates (similar as our procedure)	[12]
Clostridium strain P11	233	Hydrogenase assay on permeabilized whole cells from on syngas	[13]
Clostridium ljungdahlii	327	Hydrogenase assay on permeabilized whole cells grown on syngas	[13]
Sporomusa sphaeroides	341	Enzyme assay on purified hydrogenase from betaine grown cells	[14]

Diverse acetogens are available as pure culture. Several reviews enlisted available acetogenic strains, their ability to consume H_2 and CO_2, and their main products [7,16,13]. Although acetogens perform the same overall reaction (Eq. 1), their metabolic diversity is reflected by differences in their energy conservation strategies [17–22], leading to different H_2 thresholds, i.e. the H_2 partial pressure at which acetogenesis halts [23].

93 H_2 consumption kinetics likely also differ significantly among acetogenic strains, as different
94 doubling times or growth rates have been reported [5,8]. However, the few studies that have
95 published half-saturation coefficients for H_2 consumption by acetogens (**Table 1**), tested each
96 just one acetogenic strain. Moreover, these studies used various approaches to quantify the
97 half-saturation coefficient (**Table 1**), resulting in parameter values that are hard to compare
98 among the different studies.
99
100 With this work, we aim to investigate how the H_2 consumption rate of acetogens depends on
101 the H_2 concentration, as well as to compare the H_2 consumption kinetics of different
102 acetogens. We first measured initial H_2 consumption rates at different initial H_2 levels (ranging
103 from ~0.5 to 600 µM) for three different strains using the same pH, temperature, medium
104 and agitation. These analyses showed that H_2 consumption follows first-order kinetics, rather
105 than Monod kinetics, as no saturation was observed over the whole range of tested H_2 levels.
106 The obtained first-order rate coefficients were further validated by fitting first-order kinetics
107 on previous time-course experimental results [23]. Moreover, first-order kinetic coefficients of
108 five additional acetogens strains were also obtained by fitting time-course experimental
109 results.
110

111 **Materials and methods**

112 **Strains and culture conditions**

113 The acetogenic strains *Sporomusa ovata* (DSM 2662), *Acetobacterium woodii* (DSM 1030) and
114 *Clostridium ljungdahlii* (DSM 13528) were revived from frozen stocks in the recommended
115 medium (DSMZ 311, 135 and 879, respectively) using an organic substrate (betaine or
116 fructose). After one transfer in the same medium, when an optical density (OD_{600nm}) of
117 approximately 0.6 was reached, the cultures were filtered through a 0.2 µm polyethersulfone
118 membrane. The cells were washed three times with autotrophic growth medium inside an
119 anaerobic chamber with an N_2/CO_2 atmosphere (Jacomex, France) to remove acetate and
120 organic substrates resulting from the heterotrophic growth medium. The washed cells were
121 resuspended in autotrophic growth medium, with a composition of 1 g NH_4Cl, 0.1 g KCl, 0.8 g
122 NaCl, 0.1 g KH_2PO_4, 0.077 g $MgCl_2$, 0.02 g $CaCl_2.2H_2O$, 0.3 g L-Cysteine- $HCl.H_2O$, 20 mM
123 $NaHCO_3$, 50 mM 3-(N-morpholino) propane sulfonic acid (MOPS) brought to pH 7.0 with
124 NaOH, 0.1 g yeast extract, 10 mL vitamin solution DSMZ 141, 1 mL trace element solution and
125 0.1 mL tungstate-selenite solution per liter [24]. The strains were not grown on H_2 before the
126 start of the experiment, to avoid possible adaptations to high H_2 levels [25].

127

128 **Initial consumption rate experiment**

129 The H_2 consumption of the three acetogenic strains was characterized at a range of different
130 initial H_2 concentrations, in the same conditions of temperature, medium composition,
131 electron acceptor concentration, pH and agitation. Serum bottles (120 mL) were filled with
132 40 mL of autotrophic growth medium, while the headspace was flushed with gas mixes with
133 different H_2 concentrations (ranging from ~0.1 to 60%) and with 20% CO_2 in N_2. These gas
134 mixes were prepared using Brooks SLA5800 mass flow controllers. The serum bottles were

135 pressurized to 1.2 bar absolute pressure. At least five different H_2 initial concentrations were
136 tested in triplicate for each strain. The gas phase was allowed to equilibrate with the liquid
137 phase by agitation on an orbital shaker (Gerhardt, DE) at 100 rpm overnight at 30°C. After
138 equilibration, the bottles were inoculated with 5 mL of washed-cell suspension to reach a final
139 starting OD_{600} of 0.2. The bottles were incubated at 30°C and shaken at 100 rpm, while kept
140 upside down to avoid gas loss through the rubber septa.
141 After inoculation, the cells were given at least 1 hour of equilibration time. After that period
142 (set as time zero), samples (1.5 mL) were taken from the headspace for GC analysis until the
143 H_2 concentration had decreased by approx. 10% of the initial H_2 concentration. This allowed
144 us to measure the reaction rate at almost constant H_2 concentrations. The total pressure was
145 measured using a digital manometer (Omega DPG108, UK) before each headspace sampling.
146 The partial pressure of H_2 was calculated from the headspace H_2 concentration (%) measured
147 by GC and the total pressure at each sampling point. The concentration of dissolved H_2 in the
148 liquid phase was calculated using the Henry constant for H_2 ($7.8 \cdot 10^{-4}$ M bar^{-1}, at 30 °C) [26].
149 Abiotic controls with different initial H_2 concentrations were sampled using an identical
150 protocol to confirm that the H_2 depletion rates resulted only from the metabolic activities of
151 the acetogens. Liquid samples were taken for measurement of the OD_{600} and acetate
152 concentration in the initial and final sampling time.
153
154 **Analytical methods**
155 The analytical methods to measure the H_2 headspace concentration by GC, acetate
156 concentration by GC-VFA and the OD_{600} by spectrophotometry were previously described [23].
157 In addition, correlation curves of the cell density and dry weight with the optical density
158 (OD_{600}) were obtained for each acetogenic strain (**Table S1**). The cell density (cells mL^{-1}) was

159 quantified by Impedance Flow Cytometry (IFC) (Bactobox, SBT, Denmark). A heterotrophically
160 grown culture was washed and resuspended in autotrophic growth medium as described
161 above, and thoroughly homogenized using a vortex. Afterwards, the culture was diluted in
162 1:9 diluted Phosphate Buffer Saline (PBS) and measured in triplicates with IFC. Total cell
163 numbers were used to calculate the correlation factors. The IFC method was validated using
164 qPCR on the bacterial 16S rRNA gene, which gave results in the same order of magnitude.
165 Likewise, the dry weight was correlated to OD_{600} for each acetogenic strain in quintuplicates.
166 Cell suspensions were dried in an oven at 80°C until constant weight was reached and the
167 average dry weight was used to calculate the correlation factors.
168
169 **Determination of kinetic order and kinetic coefficients from the initial rate experiment**
170 The rate of H_2 consumption was correlated to the initial H_2 concentration to determine the
171 kinetic order. The rate of H_2 consumption was derived from the decrease of the H_2 partial
172 pressure over time. For each sampling event, the headspace pressure was measured before
173 and after sampling, to estimate the small loss of H_2 related to the withdrawal of the gaseous
174 sample. This loss of H_2 due to sampling was subtracted from the overall decrease of the H_2
175 total mole [27] to avoid overestimating the microbial consumption. The volumes of gas and
176 liquid phases were considered constant throughout the experiment. Our calculations assume
177 that H_2 was the only limiting substrate and that the agitation resulted in instantaneous
178 equilibrium between the gas and liquid phases in the bottles. The latter assumption is further
179 evaluated and discussed below.
180 H_2 consumption followed first-order kinetics over the range of H_2 concentrations evaluated
181 in this study, as described below. Since the H_2 consumption by microbial metabolism only
182 occurs in the liquid phase, but dissolved H_2 is replenished by the dissolution of gaseous H_2,

183 the first-order kinetic coefficients were calculated based on the total mole change over time,

184 similar as described previously [28]. The total moles ($n_{\mathrm{T,H2}}$) of H_2 at any time point is described

185 by Eq. 3:

186 $$n_{\mathrm{T,H_2}} = n_{\mathrm{l,H_2}} + n_{\mathrm{g,H_2}} = C_{\mathrm{H_2}} \cdot V_{\mathrm{l}} + \frac{p_{\mathrm{H_2}} \cdot V_{\mathrm{g}}}{RT} = C_{\mathrm{H_2}} \cdot \left(V_{\mathrm{l}} + \frac{V_{\mathrm{g}}}{HRT}\right) \quad (3)$$

187 With n_{l} moles in the liquid phase, n_{g} moles in the gas phase, $C_{\mathrm{H_2}}$ the H_2 concentration in the

188 liquid phase, V_{l} the volume of the liquid phase, V_{g} the volume in the gas phase, $p_{\mathrm{H_2}}$ the partial

189 pressure of H_2 in the headspace, *R* the ideal gas constant, *T* the temperature in Kelvin, *H*

190 Henry's constant of H_2 at 30 °C.

191 The ordinary differential equation describing the time dependence of the total H_2 moles in

192 the system and considering first-order kinetics reads as:

193

194 $$\frac{dn_{\mathrm{T}}}{dt} = \frac{dC_{\mathrm{H_2}}}{dt} \cdot \left(V_{\mathrm{l}} + \frac{V_{\mathrm{g}}}{HRT}\right) = -k_1\left[C_{\mathrm{H_2}} - C^*_{\mathrm{H_2}}\right] \cdot V_{\mathrm{l}} \quad (4)$$

195

196 Where k_1 is the first-order rate coefficient and has units of h^{-1} and $C^*_{\mathrm{H_2}}$ is the H_2 threshold as

197 previously experimentally determined [23]. The H_2 threshold is defined as the minimum H_2

198 dissolved concentration at which acetogenesis is thermodynamically feasible, and below

199 which acetogenesis becomes unfavorable and halts. The expression of the H_2 threshold in Eq.

200 4 is as previously proposed [10,29].

201 The first-order rate coefficients and their confidence intervals were obtained from the slope

202 of the total mol of H_2 change per time per volume of liquid culture vs the initial H_2

203 concentration (rearranging Eq. 4), using the linear regression function of GraphPad 9, which

204 also calculated the 95% confidence interval. The cell-specific first-order rate coefficients were

205 obtained by dividing k_1 by the cell density or dry weight, which was constant over the
206 experimental time.
207
208 **Determination of first-order kinetic coefficients from time course experiment**
209 To validate the first-order rate coefficients obtained from the initial rate experiment, the
210 kinetic coefficients were also calculated by numerical fitting of our previous experimental H_2
211 consumption data [23]. This study included the three strains used in the initial rate experiment,
212 as well as five additional strains: *S. ovata* (DSM 2663), *S. sphaeroides* (DSM 2875), *A. malicum*
213 (DSM 4132, *A. wieringae* (DSM 1911), and *C. autoethanogenum* (DSM 10061), for which also
214 first-order rate coefficients were fitted.
215 This earlier study [23] tested all strains at OD_{600} of 0.2 (similarly as in our initial rate experiment)
216 and used about 25 µM as starting H_2 concentration, while H_2 consumption was monitored
217 until the specific threshold was reached. In addition to these earlier experimental data, the
218 same experiment was repeated for the two *Clostridium* strains at pH 5.9 (instead of pH 7), as
219 this is closer to their optimal pH [30].
220 The first-order H_2 consumption coefficient of those eight acetogenic strains was determined
221 by fitting the above ordinary differential equation Eq. (4), on the experimental data, using the
222 starting H_2 concentration as initial condition. Eq. (4) was numerically integrated by using the
223 *ode15s* algorithm in Matlab. In addition, a non-linear Nelder-Mead simplex algorithm[31]
224 (*fminsearch*) was used to obtain the fitting curves by minimizing the sum of squares errors
225 (SSE) between the model prediction and the experimental data. Equal weight was applied to
226 all the data points for calculating SSE. The input parameters, V_l, V_g, H, R, T, and $C^*_{\mathrm{H}_2}$ were taken
227 as experimentally determined [23]. The 95% confidence interval (CI) for each predicted k_1 value
228 was further calculated as described in the **Supplementary Method 1**.

229

230 **Evaluation of mass transfer limitations**

231 The calculations described above assume instant equilibrium between the gas and liquid
232 phase. To evaluate the possible influence of mass transfer limitations on our results, we
233 calculated the overall mass transfer coefficient k_La from our orbital shaker settings, based on
234 previously reported mass transfer correlations for shakers [32] (**Supplemental Method 2**). This
235 parameter was used to evaluate whether H_2 mass transfer limitations could have impacted
236 the type of the kinetic order, observed by the initial rate experiment. Hereto, the outcome of
237 the initial rate experiment was simulated using a system of ODE's, including a term for the
238 mass transport of H_2 from the headspace to the liquid phase (**Supplemental Method 3**). The
239 outcome of an initial rate experiment was simulated assuming first-order or Monod kinetics.
240 Furthermore, the possible effect of mass transfer limitations on the fitted k_1 values was
241 assessed, by repeating the fitting of the first-order kinetic coefficients (as described above),
242 using the system of ODE's including mass transfer.

243

244 **Results**

245 **Initial consumption rates experiment (IR)**

246 H_2 consumption rates for at least five different initial H_2 concentrations were determined in
247 comparable conditions for *S. ovata*, *A. woodii* and *C. ljungdahlii*. Biological consumption was
248 confirmed by the faster depletion of H_2 than in abiotic controls under the same conditions
249 (**Figure S1**). Headspace sampling ended when the headspace H_2 concentration had decreased
250 by about 10%. In all tested conditions, the OD_{600} did not change during the short experimental
251 timeframe, as the amount of consumed H_2 was insufficient to lead to observable growth. In
252 addition, changes in the acetate concentration were insufficient to be detected.

253 Initially, H_2 consumption rates were measured up to a dissolved H_2 concentration of 180 µM
254 (approx. 20% in headspace), since the H_2 consumption rate was expected to reach a maximum
255 already in the lower µM range, based on previously reported Monod half-saturation
256 coefficients for *A. woodii* and *S. termitida* [9,11]. Plotting the experimentally determined H_2
257 consumption rates versus the dissolved H_2 concentration, however, showed a linear
258 relationship and no indication of a deflection or a maximum rate at higher H_2 concentrations
259 (**Figure 1**). For this reason, the range of initial concentrations was extended to 450 µM for *A.*
260 *woodii* and *C. ljungdahlii*, and even to 600 µM for *S. ovata*. Note that the latter concentration
261 is close to the dissolved H_2 concentration 780 µM at saturation (1 atm of pure H_2 in headspace
262 at 30 °C). Even with this extended range of initial H_2 concentration, the relationship between
263 the initial H_2 concentration and the H_2 consumption rate remained linear, for all three tested
264 strains, without any observable deflection towards a maximum (**Figure 1**). This linear
265 relationship indicates that H_2 consumption by acetogens follows first-order reaction kinetics,
266 at least at H_2 concentrations up to saturation (not considering overpressure). The absence of

267 a maximum rate at the highest H_2 concentrations suggests that H_2 consumption remains
268 limited by the H_2 concentration and not by the uptake or conversion capacity of the cells.
269 It can also be observed from **Figure 1** that *S. ovata* consumed H_2 faster at the same initial H_2
270 concentration than *A. woodii* and *C. ljungdahlii.* The slopes of the plots of **Figure 1** indeed
271 relate to the first-order rate coefficient k_1 (Eq. 4). The first-order rate coefficient is more than
272 six times higher for *S. ovata* than for *C. ljungdahlii* and almost double that for *A. woodii* (**Table**
273 **2**). *C. ljungdahlii* has the lowest k_1 among the three strains evaluated in the initial rates
274 experiment, which is most likely due to the experimental pH 7, which deviated from its
275 optimum pH 6 [30]. Also, when expressed relative to the cell density or dry weight, the cell-
276 specific first-order coefficient was highest for *S. ovata* (**Table 2**).
277
278 **Evaluation of the impact of mass transfer resistance on the kinetic order type**
279 We evaluated whether H_2 mass transfer limitations could impact the type of kinetics revealed
280 by **Figure 1.** We first estimated the overall mass transfer coefficient k_La from the
281 characteristics from our specific setup and orbital shaker settings, which was 22.7 per hour
282 (**Supplementary Methods S2**). This value was used to simulate the outcome of an initial rate
283 experiment, under the assumption of first-order or Monod kinetics. Our simulations showed
284 that our initial rate experiment revealed the true kinetic order type, as the shape of the curve
285 was not impacted by the actual mass transfer limitations (**Figure S2**). Only at a 100 times lower
286 k_La (which would correspond to static incubation), mass transfer limitations would be so
287 strong that they would lead to a linear relationship between the consumption rate and the H_2
288 concentration, also in case of Monod kinetics.
289
290

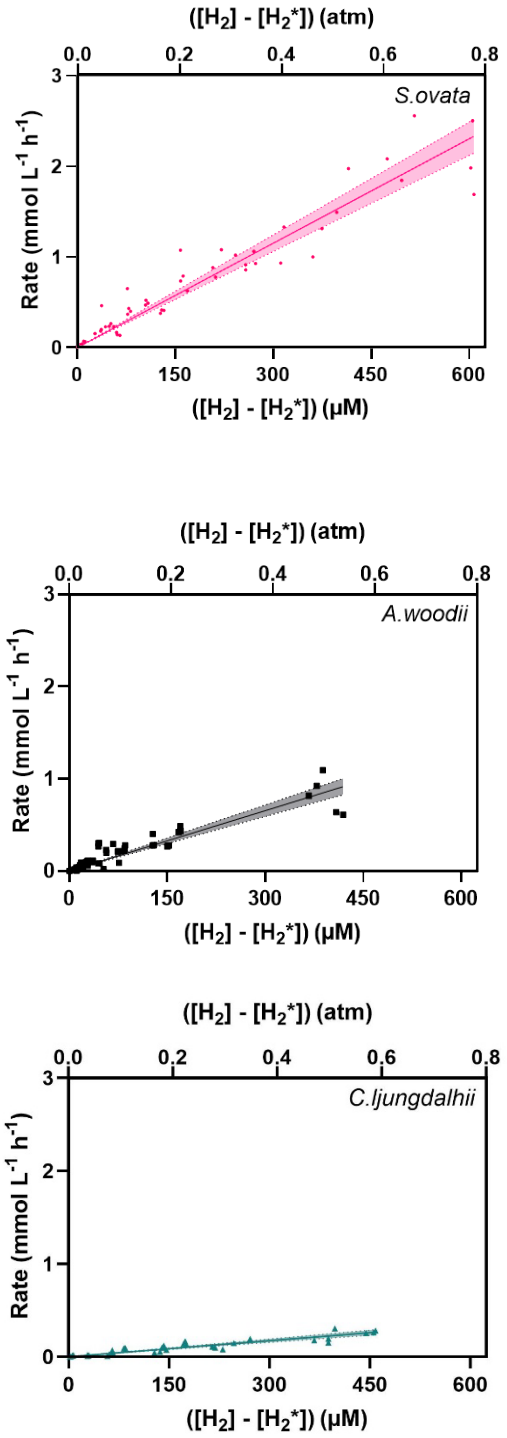

Figure 1. The observed H_2 consumption rates in function of the initial H_2 concentration for *S. ovata* (top), *A. woodii* (middle) and *C. ljungdahlii* (bottom). The observed H_2 consumption rates (*y*-axis) were expressed as total mmol H_2 per hour per L of liquid phase (Eq. 4) to account for the replenishment of H_2 from the headspace. The H_2 concentrations (*x*-axis) are corrected

297 by the H_2 threshold [23], thus the origin of the axis corresponds with the respective H_2 threshold
298 of each strain. The continuous line reflects the linear relationship as a first-order reaction. The
299 dotted line around the linear regression represents the 95% confidence interval. The liquid
300 medium is saturated with H_2 at 780 µM in our conditions. Each replicate is shown as a
301 separate dot in the plot.
302
303 **Fitting time course experiment (TC)**
304 To validate the obtained first-order rate coefficients for *S. ovata* 2662, *A. woodii* and *C.*
305 *ljungdahlii*, the kinetic coefficients were also calculated by fitting Eq. 4 on previous
306 experimental H_2 consumption time course data [23]. These independent experiments were
307 performed at the same pH, temperature, medium and agitation, but used only one initial H_2
308 concentration (~25 µM) and followed the consumption of H_2 until the H_2 threshold was
309 reached. The fitted curves described the H_2 depletion reasonably well (**Figure 2**). The k_1 values
310 obtained using the two experimental approaches are highly comparable (**Figure 3, Table 2**),
311 which validates the method used for the initial rate experiment.
312 In addition, the same fitting method was used to obtain first-order rate coefficients from
313 previous experimental results for five additional acetogenic strains, as well as from new
314 experimental H_2 depletion data for the *Clostridium* strains at pH 5.9 (**Figure 2**).
315 Among the tested strains, *A. wieringae* exhibited the highest k_1 and dry weight specific-k_1
316 (**Table 2, Figure 4, Figure S4**). Interestingly, both *S. ovata* 2662 and 2663 had significantly
317 higher k_1 values (based on both DW and cell density), compared to *A. woodii*, indicating its
318 higher overall H_2 consumption capacity under the tested conditions (**Table 2, Figure 4, Figure**
319 **S4**).

320 *C. ljungdahlii* displayed a pH-dependent k_1, with a higher value observed at its more optimal
321 pH 5.9 compared to pH 7 (**Table 2, Figure 4, Figure S4**), which aligns with the expected
322 influence of optimal growth conditions on metabolic activity. Notably, *C. ljungdahlii* also
323 demonstrated the highest cell density specific-k_1 at pH 5.9 (**Table 2, Figure S4**) of all the strains
324 tested. On the contrary, *C. autoethanogenum* did not exhibit a higher k_1 at pH 5.9 than at pH
325 7.0, even though is optimal pH is described to be 5.9 [33]. This discrepancy could relate to the
326 narrow concentration difference between the initial H_2 concentration and the H_2 threshold
327 for *C. autoethanogenum* at pH 7 (**Figure 2**), which resulted in a wide confidence interval for
328 the fitted k_1 (**Table 2**). Nevertheless, the H_2 threshold for *C. autoethanogenum* did reflect its
329 more optimal pH at 5.9 (**Figure 2**). Also *C. ljungdahlii* had a lower H_2 threshold at pH 5.9 than
330 at pH 7.0 (**Figure 2**), while in all conditions the two *Clostridium* strains still had a higher H_2
331 threshold, than all other tested strains.
332 Finally, *S. sphaeroides* displayed the lowest k_1 and biomass-specific k_1 values (DW and cell
333 density) (**Table 2**, **Figure S4**), but when analyzing the k_1 values expressed by dry weight, no
334 significant differences between *S. sphaeroides* and *A. malicum*, *A. woodii*, *C.*
335 *autoethanogenum* at pH 5.9, *Clostridium ljungdahlii* were observed (**Table 2**, **Figure 4**).
336

337 **Evaluation of the impact of mass transfer on the fitted k_1 values**

338 Our simulations (**Figure S2**) showed that the assumption of instant equilibrium between the
339 gas and liquid phase could have underestimated the actual k_1 values, which we evaluated
340 further. The overall mass transfer coefficient k_La (22.7 h^{-1}) is about four times higher than the
341 highest k_1 obtained in this study. We evaluated its influence on the fitted value of the first-
342 order rate coefficient obtained for *A. wieringae*, which is the strain with the highest
343 consumption rate and thus potentially most susceptible to mass transfer limitations. Our

344 analysis revealed that the kinetic coefficient obtained incorporating mass transfer resistance
345 is at the most 32% higher than when assuming gas-liquid equilibrium (**Figure S3**, **Table S2**).
346 For all the other strains, this difference is even lower, due to their lower k_1 (**Table S2**). As this
347 difference is much less than the difference observed between the strains (6-fold difference in
348 k_1 between highest and lowest), as well as the differences that result from other conditions
349 (for instance pH), we conclude that the results of **Table 2** (assuming instant equilibrium) are
350 sufficiently accurate and can be considered as lower limits for the H_2 consumption rates.
351

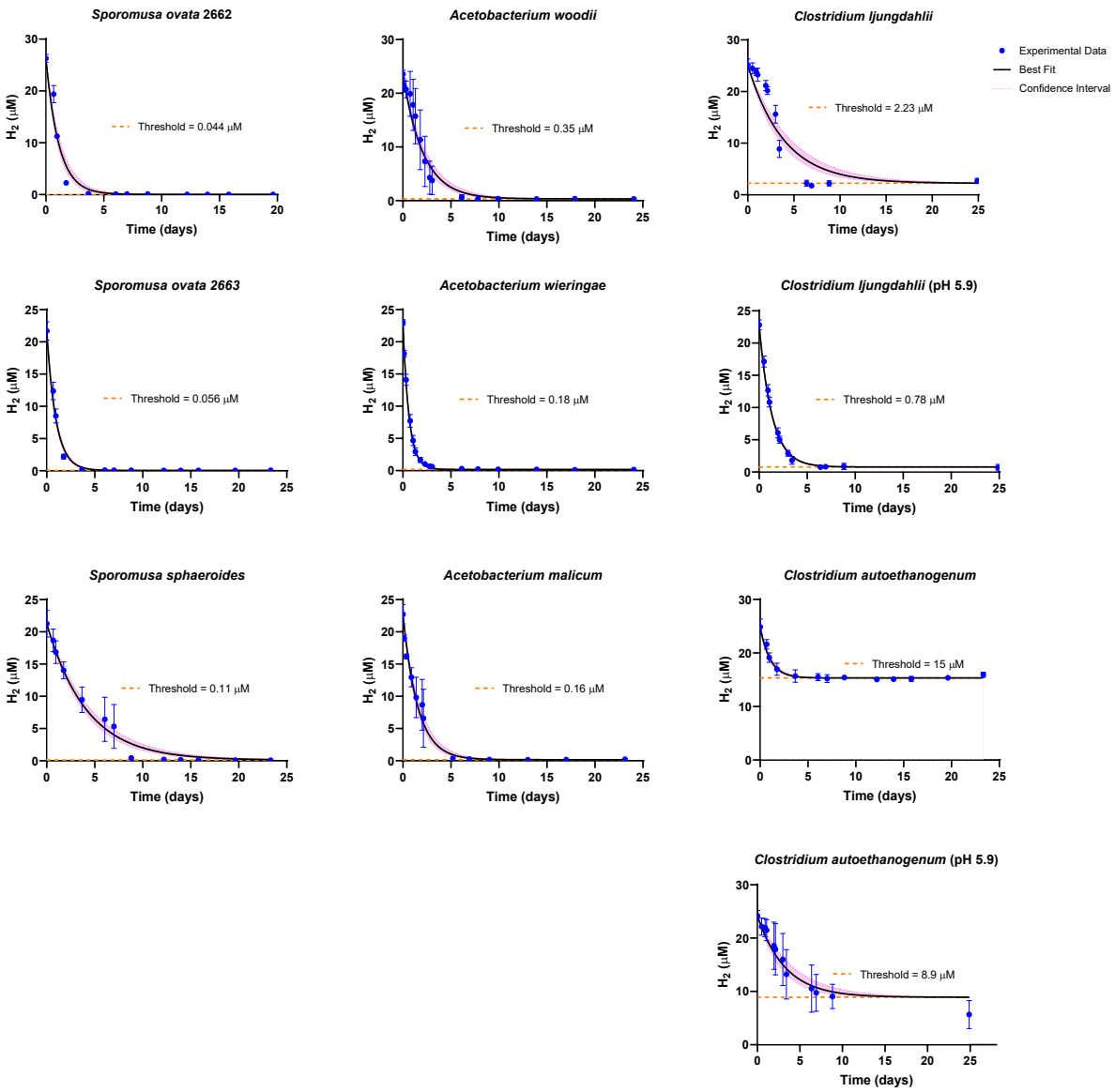

Figure 2. Best-fitting curves on the change of the dissolved H_2 concentration over time for eight acetogenic strains[23] (pH 7), as well as on similar experimental data for *C. autoethanogenum* and *C. ljungdahlii* at pH 5.9. Data points (symbols) represent the mean H_2 concentration (3 to 5 replicates) with the standard deviation given by the error bars. The best fit is given by the full black lines, while the confidence interval (95%) is aligned by pink dotted lines. The H_2 threshold is marked by a horizontal orange dotted line.

361 **Table 2.** First-order rate coefficients (k_1) of H_2 consumption obtained by the initial rates
362 experiment (IR) (grey) or by fitting the time course experiment (FT) for different acetogenic
363 bacteria. First-order rate coefficients are also given normalized by the biomass concentration,
364 expressed as cell density or as dry weight per L. All parameters are at pH 7 unless stated
365 otherwise. The 95% confidence intervals are presented in brackets next to the values. These
366 parameters were obtained under the assumption of instant equilibrium between the gas and
367 liquid phase.

368

Organism	Experiment	k_1 (h^{-1})	DW Specific k_1 (h^{-1} (g DW L^{-1})$^{-1}$)	Cell density specific k_1 x10^{-10} (h^{-1} (cell L^{-1})$^{-1}$)
S. sphaeroides	TC	0.88 (0.79 to 0.97)	10.63	0.06
C. ljungdahlii	TC	0.94 (0.79 to 1.08)	13.28	0.64
C. ljungdahlii	IR	0.58 (0.53 to 0.62)	8.19	0.25
C. autoethanogenum pH 5.9	TC	1.13 (0.87 to 1.37)	12.28	0.14
A. woodii	TC	1.74 (1.51 to 1.97)	15.47	0.39
A. woodii	IR	2.18 (2.03 to 2.33)	19.36	0.44
C. ljungdahlii pH 5.9	TC	2.76 (2.65 to 2.87)	39.02	1.11
S. ovata 2662	TC	3.27 (2.82 to 3.72)	29.81	1.09
S. ovata 2662	IR	3.84 (3.62 to 4.06)	34.97	1.21
C. autoethanogenum	TC	3.49 (3.03 to 3.95)	38.19	0.44
S. ovata 2663	TC	3.83 (3.60 to 4.06)	53.98	0.88
A. malicum	TC	2.38 (2.07 to 2.68)	13.39	0.15
A. wieringae	TC	5.79 (5.61 to 5.96)	60.93	0.67

369

370

371

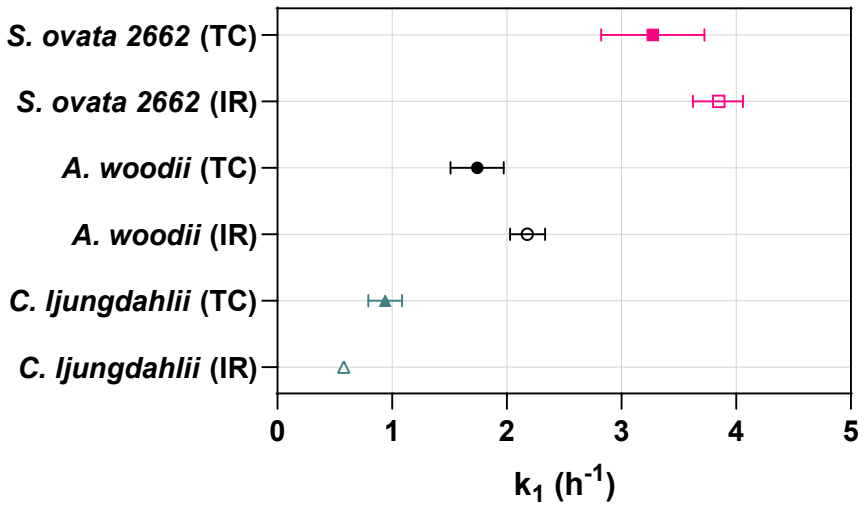

372

373 **Figure 3.** Comparative graph of the numerical values of k_1 obtained from the two

374 experimental approaches: Initial rates experiment (IR) and fitting on the time course

375 experimental data (TC) for *S. ovata* 2662, *A. woodii* and *C. ljungdahlii.* The error bar

376 corresponds to the 95% confidence interval.

377

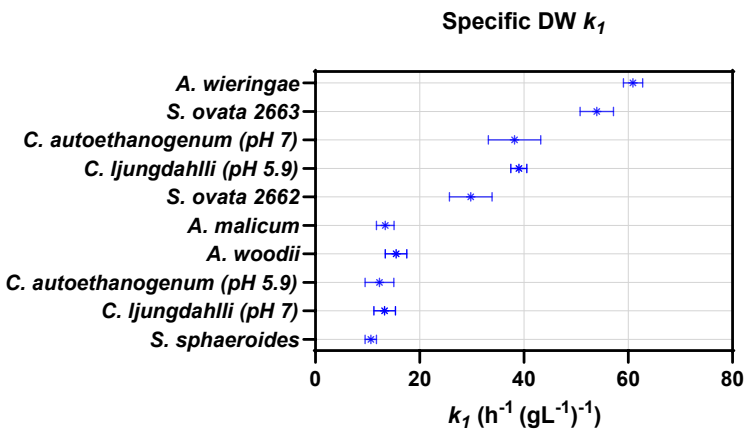

378

379 **Figure 4.** Comparison of the dry weight specific first-order coefficient k_1 obtained by fitting

380 the time course experiment for the acetogenic strains tested. The symbol represents the

381 mean value, and the bars represent the 95% confidence interval.

382

383 **Discussion**

384 **H_2 consumption by acetogens follows first-order kinetics and not Monod kinetics up to**
385 **saturated H_2 levels**

386 In this work, we found that the H_2 consumption rates of three different acetogenic strains
387 linearly increased with the dissolved H_2 concentration, up to almost saturated H_2
388 concentrations (maximal dissolved H_2 concentration was 450 to 600 µM) (**Figure 1**). This linear
389 trend shows that H_2 consumption by the different acetogenic strains followed first-order
390 kinetics. For practical reasons, we did not further increase the H_2 partial pressure, even
391 though acetogens possibly exhibit a maximum H_2 consumption rate (Monod kinetics) at
392 oversaturated H_2 concentrations. Overpressures of H_2 (>1 atm partial pressure) are relevant
393 for gas fermentation applications, but in most environmental conditions, as well as during
394 microbial electrosynthesis, only undersaturated H_2 levels (<1 atm total pressure) are
395 expected.

396 Our finding of first-order H_2 consumption kinetics contradicts with previous studies, which
397 assumed Monod kinetics (Eq. 2) and reported half-saturation coefficients for H_2 consumption
398 spanning four orders of magnitude (**Table 1**). Previously, Egli (2009)[6] pointed out that
399 determining K_s is overall difficult, even for soluble substrates, e.g. also for glucose uptake by
400 the model organism *E. coli*, reported K_s values range over three orders of magnitude. Egli
401 (2009)[6] related this to differences in the experimental approach. In addition, the use of
402 growth rates is problematic, as changes in biomass are hard to measure at low substrate
403 concentrations [6]. Also Robinson and Tiedje (1982)[34] pointed out that underestimated H_2 half-
404 saturation coefficients can result from relating H_2 consumption to growth. Consequently, the
405 direct determination of the consumption rate in function of the substrate concentration, as
406 in our study, reduces the associated error.

407 The previous studies reporting half-saturation coefficients for acetogenic H_2 consumption
408 (**Table 1**) did not report the reliability of their K_s value. Smith *et al*. (2020) [29] clearly illustrated
409 the importance of reporting the confidence interval of parameter estimates. They found that
410 both Monod kinetics and first-order kinetics fitted batch growth data for the acetogen *Blautia*
411 *hydrogenotrophica* well, but described that in the case of Monod kinetics, the values of K_s and
412 μ_{max} were strongly correlated, which was reflected by an extremely wide confidence interval
413 for K_s. In contrast, they reported a narrow confidence interval for their first-order rate
414 coefficient. In our work, the confidence intervals associated with the first-order kinetic
415 coefficient are also narrow (**Table 2**). In addition, we applied two different experimental
416 approaches (initial rate experiment and fitting time course data), which resulted in highly
417 comparable k_1 values (**Figure 3**). Our k_1 values can thus be considered as highly reliable.
418 Possibly, H_2 mass transfer limitations affect the observed H_2 consumption kinetic order type
419 [35,36]. Through simulations (**Figure S2**), we showed that the actual mass transfer resistance in
420 our system could not have masked the true kinetic order type. The mass transfer limitations
421 did affect the estimated k_1 values, but this was maximally 32% for the strain with the highest
422 k_1 (**Figure S3**, **Table S2**).
423 Besides Smith *et al*. (2020) [29], few other studies previously found indications for first-order H_2
424 consumption by acetogens. For instance, a study of *A. woodii* in chemostats to determine its
425 maximal H_2 uptake rate concluded that a physiological limitation was likely not reached in
426 their experiments [37]. Also the relatively high K_s found using several hydrogenase assays (**Table**
427 **1**), show that the maximum H_2 conversion rate was not reached below saturation.
428
429 **First-order H_2 consumption rate coefficients differ up to six times among acetogenic strains**

430 Our results demonstrate that acetogenic strains strongly differ in their first-order H_2
431 consumption rate coefficient (**Table 2**, **Figure 4**). The highest k_1 coefficient was obtained for
432 *A. wieringae*, which had a six-fold higher consumption rate than *S. sphaeroides,* for which the
433 lowest k_1 value was found. The same strains have respectively the highest and lowest k_1 value
434 when k_1 is expressed per dry weight. *C. ljungdahlii* at pH 5.9 had one of the highest k_1
435 expressed per cell density, but an average k_1 expressed per dry weight. This discrepancy likely
436 stems from cell size differences, as *C. ljungdahlii* possibly has larger cells, corresponding to
437 fewer cells per unit of dry weight.
438 Contrary to what was previously observed for H_2 thresholds [23], k_1 values did not correlate with
439 the genus, indicating that k_1 values might be strain-specific. Likewise, Groher and Weuster-
440 Botz [8] described variations in the maximal H_2 uptake rate and maximal growth rate among
441 three *Acetobacterium* and two *Sporomusa* species. Differences in growth rates at comparable
442 conditions within the same genus were also observed by Bengelsdorf *et al*. 2016 [38] for four
443 different *Clostridium* strains.
444 In part, these variations in k_1 are likely due to differences in optimal conditions, as illustrated
445 by the different k_1 values at different pH for the *Clostridium* strains (**Table 2**, **Figure 4**). Besides
446 pH, the H_2 consumption rate of a single acetogenic strain varies with the temperature [10] and
447 the medium composition. For example, differences in the concentrations of yeast extract,
448 reductive agents or trace elements (selenium and tungsten) are known to affect acetogenesis
449 rates [39–41].
450 In addition to varying optimal conditions, differences in H_2 consumption rates between
451 acetogenic strains could be due to different kinetics of the involved hydrogenases, which are
452 the metalloenzymes catalyzing the redox conversion between H_2 and protons. The
453 hydrogenases type [NiFe] and the [FeFe] hydrogenases are commonly found in acetogens [42–

454 [44]. These enzymes exhibit complex structural features, including hydrophobic channels for gas
455 diffusion to the active site [45]. This structural conformation can influence the affinity and the
456 sensitivity of the enzyme [46]. Indeed, some studies already demonstrated differences in the
457 hydrogenase kinetics of different acetogens [13,15,47].
458 In our study, *A. wieringae* exhibited the highest H_2 consumption rate under our experimental
459 conditions, followed by *S. ovata* and the two *Clostridium* strains (**Table 2**, **Figure 4**). Numerous
460 studies already explored the capabilities of *C. ljungdahlii* and *C. autoethanogenum* as catalysts
461 in gas conversion technologies [48–52], because their high conversion rates. Maybe less known,
462 but also *A. wieringae* has already been recognized for its high conversion rates on C_1 carbon
463 sources [53,54]. In addition, *A. wieringae* was the keystone member in an enriched microbial
464 community leading to high rates of microbial electrosynthesis [55,56], making it a highly
465 promising strain for applications.
466
467 **Implications**
468 Our finding that H_2 consumption by acetogens follows first-order kinetics up to almost
469 saturated H_2 levels, means that the dissolved H_2 concentration is a major factor limiting
470 acetogenesis in both environmental and biotechnological systems. First-order kinetics entails
471 that the rate of H_2 conversion per unit biomass is higher at an increased dissolved H_2
472 concentration (Eq. 4). This insight is highly relevant to optimize acetogenic biotechnologies.
473 In gas fermentation, increasing the H_2 partial pressure is often used to increase the H_2
474 solubility and thus to overcome mass transfer resistance[57]. Our results suggest that this also
475 leads to higher consumption rates by acetogens. In contrast, low dissolved H_2 levels often
476 prevail in microbial electrosynthesis systems, which likely contributes to their limited acetate
477 production rates [58].

478 In addition, the understanding that H_2 consumption by acetogens follows first-order kinetics
479 is important to understand their relevance in environmental settings. For instance,
480 competition between acetogenic bacteria and methanogenic archaea has mostly been
481 studied by comparing their Monod kinetic parameters for H_2 consumption [10,59], but the use
482 of the right kinetic order could lead to more accurate interpretations. Furthermore, to
483 understand acetogenesis in both natural and biotechnological settings, numerical simulations
484 are highly interesting, but the value of models entirely depends on the use of the correct
485 expressions and parameter values governing acetogenic kinetics. Consequently, the insights
486 generated by our study are of high relevance for any research related to acetogenesis.
487 This work also showed that first-order rate coefficients between acetogens differ up to six
488 times (**Table 2**, **Figure 4**). The k_1 values obtained by this work are of high value for optimal
489 strain selection for the different biotechnological applications. Nowadays, acetogenic strain
490 selection is mostly based on the desired end-product. However, genetic engineering can alter
491 the formed end-product [54,60,61], while H_2 consumption and product formation rates are much
492 harder to engineer. Consequently, it remains important to understand the intrinsic
493 differences in kinetics between the available acetogenic strains to allow optimal strain
494 selection.
495 Finally, it should be noted that this work only characterized H_2 consumption rates. This work
496 did not analyze growth nor acetate production rates. Moreover, the H_2 consumption rate
497 does not only depend on the (biomass specific) k_1, but definitely also on the biomass density
498 in the system, which in turn depends on growth. Acetogens likely differ in their growth yields,
499 as they have different ATP gains [23]. Furthermore, product versus biomass yields might vary
500 among acetogens. Insights into all these aspects are required, before a comprehensive
501 understanding of the product and growth kinetics of acetogens becomes possible.

502 **Author contributions**

503 LM and JP designed the experiments; LM performed the experimental work; SC fitted the k_1
504 values on our experimental results; MFB performed qPCR; JC performed the simulations
505 investigating mass transfer limitations; LM and LVG analyzed the experimental data; LM and
506 SC constructed the figures; LM and JP wrote the manuscript; SC, FMB, LVG and JC edited the
507 manuscript; JC and JP acquired funding and performed supervision. All authors contributed
508 to the article and approved the submitted version.

509

510 **Acknowledgements**

511 This work was financed by a starting grant of Aarhus Universitets Forskningsfond (AUFF), as
512 well as by a Green Transition Project I grant (MES-MODEL, 1127-00048B) from the
513 Independent Research Fund Denmark (DFF).

514 We thank Lars-Erik Meyer for his advice on how to determine kinetics. We also thank Thomas
515 Thomas Dyekjær, Cecilie Nielsen, Gitte Hastrup and Heidi Skov Johansen for their technical
516 and practical support of this project. Miguel Oliveira is acknowledged for his contribution to
517 the Bactobox setup.

518

519 **References**

520 (1) Basen, M.; Müller, V. Editorial: Acetogens - from the Origin of Life to Biotechnological
521 Applications. *Frontiers in Microbiology*. Frontiers Media S.A. 2023.
522 https://doi.org/10.3389/fmicb.2023.1186930.

523 (2) Smith, N. W.; Shorten, P. R.; Altermann, E.; Roy, N. C.; McNabb, W. C. Competition for
524 Hydrogen Prevents Coexistence of Human Gastrointestinal Hydrogenotrophs in
525 Continuous Culture. *Front Microbiol* **2020**, *11*.
526 https://doi.org/10.3389/fmicb.2020.01073.

527 (3) Drake, H. L.; Küsel, K.; Matthies, C. Ecological Consequences of the Phylogenetic and
528 Physiological Diversities of Acetogens. *Antonie van Leeuwenhoek, International Journal*
529 *of General and Molecular Microbiology* **2002**, *81* (1–4), 203–213.
530 https://doi.org/10.1023/A:1020514617738.

531 (4) Harnisch, F.; Deutzmann, J. S.; Boto, S. T.; Rosenbaum, M. A. Microbial Electrosynthesis:
532 Opportunities for Microbial Pure Cultures. *Trends Biotechnol* **2024**.
533 https://doi.org/10.1016/j.tibtech.2024.02.004.

534 (5) Philips, J. Extracellular Electron Uptake by Acetogenic Bacteria: Does H_2 Consumption
535 Favor the H_2 Evolution Reaction on a Cathode or Metallic Iron ? *Front Microbiol* **2020**,
536 *10*, 1–13. https://doi.org/10.3389/fmicb.2019.02997.

537 (6) Egli, T. Growth Kinetics, Bacterial. In *Encyclopedia of Microbiology*; Elsevier Inc., 2009;
538 pp 180–193. https://doi.org/10.1016/B978-012373944-5.00260-1.

539 (7) Bengelsdorf, F. R.; Beck, M. H.; Erz, C.; Hoffmeister, S.; Karl, M. M.; Riegler, P.; Wirth,
540 S.; Poehlein, A.; Weuster-Botz, D.; Dürre, P. Bacterial Anaerobic Synthesis Gas (Syngas)
541 and CO_2 + H_2 Fermentation. *Adv Appl Microbiol* **2018**, *103*, 143–221.
542 https://doi.org/10.1016/BS.AAMBS.2018.01.002.

543 (8) Groher, A.; Weuster-Botz, D. Comparative Reaction Engineering Analysis of Different
544 Acetogenic Bacteria for Gas Fermentation. *J Biotechnol* **2016**, *228*, 82–94.
545 https://doi.org/10.1016/j.jbiotec.2016.04.032.

546 (9) Peters, V.; Janssen, P. H.; Conrad, R. Efficiency of Hydrogen Utilization during
547 Unitrophic and Mixotrophic Growth of *Acetobacterium Woodii* on Hydrogen and
548 Lactate in the Chemostat. *FEMS Microbiol Ecol* **1998**, *26*, 317–324.
549 https://doi.org/10.1111/j.1574-6941.1998.tb00516.x.

550 (10) Kotsyurbenko, O. R.; Glagolev, M. V.; Nozhevnikova, A. N.; Conrad, R. Competition
551 between Homoacetogenic Bacteria and Methanogenic Archaea for Hydrogen at Low
552 Temperature. *FEMS Microbiol Ecol* **2001**, *38* (2–3), 153–159.
553 https://doi.org/10.1016/S0168-6496(01)00179-9.
554 (11) Breznak, J. A.; Switzer, J. M.; Seitz, H.-J. Sporomusa Termitida Sp. Nov., an H2/CO2-
555 Utilizing Acetogen Isolated from Termites. *Arch Microbiol* **1988**, *50*, 282–288.
556 (12) Genthner, B. R.; Bryant, M. P. *Additional Characteristics of One-Carbon-Compound*
557 *Utilization by Eubacterium Limosum and Acetobacterium Woodii*; 1987.
558 (13) Skidmore, B. E.; Baker, R. A.; Banjade, D. R.; Bray, J. M.; Tree, D. R.; Lewis, R. S. Syngas
559 Fermentation to Biofuels: Effects of Hydrogen Partial Pressure on Hydrogenase
560 Efficiency. **2013**. https://doi.org/10.1016/j.biombioe.2013.01.034.
561 (14) Dobrindt, U.; Ulrich, M. Purification and Characterization of a Membrane-Bound
562 hydrogenase from Sporomusa Sphaeroides involved in Energy-Transducing Electron
563 Transport. *Arch Microbiol* **1996**, *165*, 141–147.
564 (15) Ragsdale, S. W.; Ljungdahl, L. G. Hydrogenase from Acetobacterium Woodii*. *Arch*
565 *Microbiol* **1984**, *139*, 361–365.
566 (16) Schiel-Bengelsdorf, B.; Dürre, P. Pathway Engineering and Synthetic Biology Using
567 Acetogens. *FEBS Lett* **2012**, *586*, 2191–2198.
568 https://doi.org/10.1016/j.febslet.2012.04.043.
569 (17) Wiechmann, A.; Müller, V. Energy Conservation in the Acetogenic Bacterium
570 Clostridium Aceticum. *Microorganisms* **2021**, *9* (2), 1–12.
571 https://doi.org/10.3390/microorganisms9020258.
572 (18) Katsyv, A.; Müller, V. Overcoming Energetic Barriers in Acetogenic C1 Conversion.
573 *Frontiers in Bioengineering and Biotechnology | www.frontiersin.org* **2020**, *8*, 621166.
574 https://doi.org/10.3389/fbioe.2020.621166.
575 (19) Rosenbaum, F. P.; Müller, V. Energy Conservation under Extreme Energy Limitation:
576 The Role of Cytochromes and Quinones in Acetogenic Bacteria. *Extremophiles* **2021**,
577 *25*, 413–424. https://doi.org/10.1007/s00792-021-01241-0.
578 (20) Kremp, F.; Roth, J.; Müller, V. A Third Way of Energy Conservation in Acetogenic
579 Bacteria. *Microbiol Spectr* **2022**.

580 (21) Kremp, F.; Roth, J.; Müller, V. The *Sporomusa* Type Nfn Is a Novel Type of Electron-
581 Bifurcating Transhydrogenase That Links the Redox Pools in Acetogenic Bacteria. *Sci*
582 *Rep* **2020**, *10* (1). https://doi.org/10.1038/S41598-020-71038-2.
583 (22) Wiechmann, A.; Ciurus, S.; Oswald, F.; Seiler, V. N.; Volker Müller, •. It Does Not Always
584 Take Two to Tango: "Syntrophy" via Hydrogen Cycling in One Bacterial Cell. *ISME J*
585 **2020**, *14*, 1561–1570. https://doi.org/10.1038/s41396-020-0627-1.
586 (23) Munoz, L.; Philips, J. No Acetogen Is Equal: Strongly Different H2 Thresholds Reflect
587 Diverse Bioenergetics in Acetogenic Bacteria. *Environ Microbiol* **2023**, *25* (10), 2032–
588 2040. https://doi.org/10.1111/1462-2920.16429.
589 (24) Patil, S. A.; Arends, J. B. A.; Vanwonterghem, I.; Van Meerbergen, J.; Guo, K.; Tyson, G.
590 W.; Rabaey, K. Selective Enrichment Establishes a Stable Performing Community for
591 Microbial Electrosynthesis of Acetate from CO_2. *Environ Sci Technol* **2015**, *49* (14),
592 8833–8843. https://doi.org/10.1021/es506149d.
593 (25) Kato, S.; Yumoto, I.; Kamagata, Y. Isolation of Acetogenic Bacteria That Induce
594 Biocorrosion by Utilizing Metallic Iron as the Sole Electron Donor. *Appl Environ*
595 *Microbiol* **2015**, *81* (1), 67–73. https://doi.org/10.1128/AEM.02767-14.
596 (26) Sander, R. Compilation of Henry's Law Constants (Version 4.0) for Water as Solvent.
597 *Atmos. Chem. Phys* **2015**, *15*, 4399–4981. https://doi.org/10.5194/acp-15-4399-2015.
598 (27) Dopffel, N.; Mayers, K.; Kedir, A.; Alagic, E.; Annie An-Stepec, B.; Djurhuus, K.; Boldt, D.;
599 Beeder, J.; Hoth, S. Microbial Hydrogen Consumption Leads to a Significant PH Increase
600 under High-Saline-Conditions: Implications for Hydrogen Storage in Salt Caverns.
601 *Scientific Reports* **2023**, *13*. https://doi.org/10.1038/s41598-023-37630-y.
602 (28) Karadagli, F.; Rittmann, B. E. Thermodynamic and Kinetic Analysis of the H_2 Threshold
603 for *Methanobacterium Bryantii* M.o.H. *Biodegradation* **2007**, *18* (4), 439–452.
604 https://doi.org/10.1007/s10532-006-9073-7.
605 (29) Smith, N. W.; Shorten, P. R.; Altermann, E.; Roy, N. C.; Mcnabb, W. C. Mathematical
606 Modelling Supports the Existence of a Threshold Hydrogen Concentration and Media-
607 Dependent Yields in the Growth of a Reductive Acetogen. *Bioprocess Biosyst Eng* **2020**,
608 *43*, 885–894. https://doi.org/10.1007/s00449-020-02285-w.
609 (30) Tanner, R. S.; Miller, L. M.; Decheng, A. *Clostridium Ljungdahlii Sp. Nov., an Acetogenic*
610 *Species in Clostridial RRNA Homology Group I*; 1993; Vol. 43.

611 (31) Lagarias, J. C.; Reeds, J. A.; Wright, M. H.; Wright, P. E.; Optim, S. J. *CONVERGENCE*
612 *PROPERTIES OF THE NELDER-MEAD SIMPLEX METHOD IN LOW DIMENSIONS **; 1998;
613 Vol. 9, pp 112–147. http://www.siam.org/journals/siopt/9-1/30347.html.
614 (32) Klöckner, W.; Büchs, J. Advances in Shaking Technologies. *Trends in Biotechnology*.
615 June 2012, pp 307–314. https://doi.org/10.1016/j.tibtech.2012.03.001.
616 (33) Abrini, J.; Naveau, H.; Nyns, E.-J. *Clostridium Autoethanogenum, Sp. Nov., an Anaerobic*
617 *Bacterium That Produces Ethanol from Carbon Monoxide*; 1994; Vol. 161.
618 (34) Robinson, J. A.; Tiedje, J. M. Kinetics of Hydrogen Consumption by Rumen Fluid,
619 Anaerobic Digestor Sludge, and Sedimentt. *Appl Environ Microbiol* **1982**, *44* (6), 1374–
620 1384.
621 (35) Karadagli Andrew Marcus Bruce E Rittmann, F. K. Role of Hydrogen (H 2) Mass Transfer
622 in Microbiological H 2-Threshold Studies. *Biodegradation* **2019**, *30*, 113–125.
623 https://doi.org/10.1007/s10532-019-09870-1.
624 (36) Robinson, J. A.; Tiedje, J. M. *Nonlinear Estimation of Monod Growth Kinetic Parameters*
625 *from a Single Substrate Depletion Curve*; 1983; Vol. 45.
626 https://journals.asm.org/journal/aem.
627 (37) Novak, K.; Neuendorf, C. S.; Kofler, I.; Kieberger, N.; Klamt, S.; Pflügl, S. Blending
628 Industrial Blast Furnace Gas with H2 Enables Acetobacterium Woodii to Efficiently Co-
629 Utilize CO, CO2 and H2. *Bioresour Technol* **2021**, *323*.
630 https://doi.org/10.1016/j.biortech.2020.124573.
631 (38) Bengelsdorf, F. R.; Poehlein, A.; Linder, S.; Erz, C.; Hummel, T.; Hoffmeister, S.; Daniel,
632 R.; Dürre, P. Industrial Acetogenic Biocatalysts: A Comparative Metabolic and Genomic
633 Analysis. *Front Microbiol* **2016**, *7* (JUL). https://doi.org/10.3389/fmicb.2016.01036.
634 (39) An, T.; Kim, Y. K. Effect of Selenium and Tungsten on Cell Growth and Metabolite
635 Production in Syngas Fermentation Using "Clostridium Autoethanogenum." *J*
636 *Biotechnol* **2022**, *356*, 60–64. https://doi.org/10.1016/j.jbiotec.2022.07.004.
637 (40) Lanzillo, F.; Pisacane, S.; Raganati, F.; Russo, M. E.; Salatino, P.; Marzocchella, A.
638 Optimization of CO Fermentation by Clostridium Carboxidivorans in Batch Reactors:
639 Effects of the Medium Composition. *Anaerobe* **2024**, *87*.
640 https://doi.org/10.1016/j.anaerobe.2024.102855.

641 (41) Groher, A.; Weuster-Botz, D. General Medium for the Autotrophic Cultivation of
642 Acetogens. *Bioprocess Biosyst Eng* **2016**, *39* (10), 1645–1650.
643 https://doi.org/10.1007/s00449-016-1634-5.
644 (42) Schuchmann, K.; Chowdhury, N. P.; Müller, V. Complex Multimeric [FeFe]
645 Hydrogenases: Biochemistry, Physiology and New Opportunities for the Hydrogen
646 Economy. *Front Microbiol* **2018**, *9*. https://doi.org/10.3389/fmicb.2018.02911.
647 (43) Madjarov, J.; Soares, R.; Paquete, C. M.; Louro, R. O. *Sporomusa Ovata* as Catalyst for
648 Bioelectrochemical Carbon Dioxide Reduction : A Review across Disciplines from
649 Microbiology to Process Engineering. *Front Microbiol* **2022**, *13*, 1–13.
650 https://doi.org/10.3389/fmicb.2022.913311.
651 (44) Peters, J. W.; Schut, G. J.; Boyd, E. S.; Mulder, D. W.; Shepard, E. M.; Broderick, J. B.;
652 King, P. W.; Adams, M. W. W. [FeFe]- and [NiFe]-Hydrogenase Diversity, Mechanism,
653 and Maturation. *Biochimica et Biophysica Acta - Molecular Cell Research*. Elsevier June
654 1, 2015, pp 1350–1369. https://doi.org/10.1016/j.bbamcr.2014.11.021.
655 (45) Zacarias, S.; Temporão, A.; Barrio, M. Del; Fourmond, V.; Léger, C.; Matias, P. M.;
656 Pereira, I. A. C. A Hydrophilic Channel Is Involved in Oxidative Inactivation of a [NiFeSe]
657 Hydrogenase. *ACS Catal* **2019**, *9* (9), 8509–8519.
658 https://doi.org/10.1021/acscatal.9b02347.
659 (46) Leroux, F.; Bastien Dementin, S.; Né Dicte Burlat, B.; Cournac, L.; Volbeda, A.; Phanie
660 Champ, S.; Martin, L.; Guigliarelli, B.; Bertrand, P.; Fontecilla-Camps, J.; Rousset, M.; Lé,
661 C. *Experimental Approaches to Kinetics of Gas Diffusion in Hydrogenase*; 2008.
662 www.pnas.orgcgidoi10.1073pnas.0803689105.
663 (47) Daniel, S. L.; Hsu, T.; Dean, S. I.; Drake, H. L. *Characterization of the H2-and CO-*
664 *Dependent Chemolithotrophic Potentials of the Acetogens Clostridium*
665 *Thermoaceticum and Acetogenium Kivuit*; 1990; Vol. 172.
666 https://journals.asm.org/journal/jb.
667 (48) Zhu, H.-F.; Liu, Z.-Y.; Zhou, X.; Yi, J.-H.; Lun, Z.-M.; Wang, S.-N.; Tang, W.-Z.; Li, F.-L.
668 Energy Conservation and Carbon Flux Distribution During Fermentation of CO or
669 H2/CO2 by Clostridium Ljungdahlii. *Front Microbiol* **2020**, *11*.
670 https://doi.org/10.3389/fmicb.2020.00416.
671 (49) Bardone, E.; Marzocchella, A.; Keshavarz, T.; Stoll, K. I.; Herbig, S.; Zwick, M.; Boukis,
672 N.; Sauer, J.; Neumann, A.; Oswald, F. Fermentation of H2 and CO2 with Clostridium

Ljungdahlii at Elevated Process Pressure-First Experimental Results. *Chem Eng Trans* **2018**, *64*. https://doi.org/10.3303/CET1864026.

(50) Boto, S. T.; Bardl, B.; Harnisch, F.; Rosenbaum, M. A. Microbial Electrosynthesis with Clostridium Ljungdahlii Benefits from Hydrogen Electron Mediation and Permits a Greater Variety of Products †. **2023**. https://doi.org/10.1039/d3gc00471f.

(51) Martínez-Ruano, J.; Suazo, A.; Véliz, F.; Otálora, F.; Conejeros, R.; González, E.; Aroca, G. Electro-Fermentation with Clostridium Autoethanogenum: Effect of PH and Neutral Red Addition. *Environ Technol Innov* **2023**, *31*. https://doi.org/10.1016/j.eti.2023.103183.

(52) Valgepea, K.; Talbo, G.; Takemori, N.; Takemori, A.; Ludwig, C.; Mahamkali, V.; Mueller, A. P.; Tappel, R.; Köpke, M.; Simpson, S. D.; Nielsen, L. K.; Marcellin, E. Absolute Proteome Quantification in the Gas-Fermenting Acetogen Clostridium Autoethanogenum . *mSystems* **2022**, *7* (2). https://doi.org/10.1128/msystems.00026-22.

(53) Arantes, A. L.; Moreira, J. P. C.; Diender, M.; Parshina, S. N.; Stams, A. J. M.; Alves, M. M.; Alves, J. I.; Sousa, D. Z. Enrichment of Anaerobic Syngas-Converting Communities and Isolation of a Novel Carboxydotrophic Acetobacterium Wieringae Strain JM. *Front Microbiol* **2020**, *11* (January). https://doi.org/10.3389/fmicb.2020.00058.

(54) Moreira, J. P. C.; Heap, J. T.; Alves, J. I.; Domingues, L. Developing a Genetic Engineering Method for Acetobacterium Wieringae to Expand One-Carbon Valorization Pathways. *Biotechnology for Biofuels and Bioproducts* **2023**, *16* (1). https://doi.org/10.1186/s13068-023-02259-6.

(55) Marshall, C. W.; Ross, D. E.; Handley, K. M.; Weisenhorn, P. B.; Edirisinghe, J. N.; Henry, C. S.; Gilbert, J. A.; May, H. D.; Norman, & R. S. Metabolic Reconstruction and Modeling Microbial Electrosynthesis. **2017**, *7* (839). https://doi.org/10.1038/s41598-017-08877-z.

(56) Mills, S.; Dessì, P.; Pant, D.; Farràs, P.; Sloan, W. T.; Collins, G.; Zeeshan Ijaz, U. A Meta-Analysis of Acetogenic and Methanogenic Microbiomes in Microbial Electrosynthesis. *NPJ Biofilms Microbiomes* **2022**, *8* (73). https://doi.org/10.1038/s41522-022-00337-5.

(57) Van Hecke, W.; Bockrath, R.; De Wever, H. Effects of Moderately Elevated Pressure on Gas Fermentation Processes. *Bioresource Technology*. Elsevier Ltd December 1, 2019. https://doi.org/10.1016/j.biortech.2019.122129.

(58) Prévoteau, A.; Carvajal-Arroyo, J. M.; Ganigué, R.; Rabaey, K. Microbial Electrosynthesis from CO2: Forever a Promise? *Curr Opin Biotechnol* **2020**, *62*, 48–57. https://doi.org/10.1016/j.copbio.2019.08.014.

(59) Tsapekos, P. ; Alvarado-Morales, M. ;; Angelidaki, I. H2 Competition between Homoacetogenic Bacteria and Methanogenic Archaea during Biomethanation from a Combined Experimental-Modelling Approach. *J Environ Chem Eng* **2022**, *10* (2). https://doi.org/10.1016/j.jece.2022.107281.

(60) Tremblay, P.-L.; Zhang, T. Genetic Tools for the Electrotroph Sporomusa Ovata and Autotrophic Biosynthesis. *Biotechnology | Full-Length Text* **2023**. https://doi.org/10.1128/aem.01757-23.

(61) Bourgade, B.; Minton, N. P.; Islam, M. A. Genetic and Metabolic Engineering Challenges of C1-Gas Fermenting Acetogenic Chassis Organisms. *FEMS Microbiol Rev* **2021**, *008*, 1–20. https://doi.org/10.1093/femsre/fuab008.